micromachines

Article

Effects of Proton Irradiation on the Current Characteristics of SiN-Passivated AlGaN/GaN MIS-HEMTs Using a TMAH-Based Surface Pre-Treatment

Young Jun Yoon [1], Jae Sang Lee [1], Jae Kwon Suk [1], In Man Kang [2], Jung Hee Lee [2], Eun Je Lee [3] and Dong Seok Kim [1,*]

[1] Korea Multi-Purpose Accelerator Complex, Korea Atomic Energy Research Institute, Gyeongju 38180, Korea; yjyoon@kaeri.re.kr (Y.J.Y.); jslee8@kaeri.re.kr (J.S.L.); jksuk@kaeri.re.kr (J.K.S.)
[2] School of Electronic and Electric Engineering, Kyungpook National University, Daegu 41566, Korea; imkang@ee.knu.ac.kr (I.M.K.); jlee@ee.knu.ac.kr (J.H.L.)
[3] Advanced Radiation Technology Institute, Korea Atomic Energy Research Institute, Jeongeup 56212, Korea; leeeunje@kaeri.re.kr
* Correspondence: dongseokkim@kaeri.re.kr; Tel.: +82-054-750-5310

Abstract: This study investigated the combined effects of proton irradiation and surface pre-treatment on the current characteristics of Gallium Nitride (GaN)-based metal-insulator-semiconductor high-electron-mobility-transistors (MIS-HEMTs) to evaluate the radiation hardness involved with the Silicon Nitride (SiN) passivation/GaN cap interface. The impact of proton irradiation on the static and dynamic current characteristics of devices with and without pre-treatment were analyzed with 5 MeV proton irradiation. In terms of transfer characteristics before and after the proton irradiation, the drain current of the devices without and with pre-treatment were reduced by an increase in sheet and contact resistances after the proton irradiation. In contrast with the static current characteristics, the gate-lag characteristics of the device with pre-treatment were significantly degenerated. In the device with pre-treatment, the hydrogen passivation for surface states of the GaN cap was formed by the pre-treatment and SiN deposition processes. Since the hydrogen passivation was removed by the proton irradiation, the newly created vacancies resulted in the degeneration of gate-lag characteristics. After nine months in an ambient atmosphere, the gate-lag characteristics of the device with pre-treatment were recovered because of the hydrogen recombination. These results demonstrated that the radiation hardness of MIS-HEMTs was affected by the SiN/GaN interface quality.

Keywords: Gallium Nitride (GaN); proton irradiation; surface pre-treatment

check for updates

Citation: Yoon, Y.J.; Lee, J.S.; Suk, J.K.; Kang, I.M.; Lee, J.H.; Lee, E.J.; Kim, D.S. Effects of Proton Irradiation on the Current Characteristics of SiN-Passivated AlGaN/GaN MIS-HEMTs Using a TMAH-Based Surface Pre-Treatment. *Micromachines* **2021**, *12*, 864. https://doi.org/10.3390/mi12080864

Academic Editor: Giovanni Verzellesi

Received: 5 July 2021
Accepted: 22 July 2021
Published: 23 July 2021

1. Introduction

Gallium Nitride (GaN)-based devices have received attention for high-frequency and high-power applications due to their outstanding characteristics, such as low on-resistance (R_{on}) and high speed, which can be realized by two-dimensional electron gas (2DEG), formed by a AlGaN/GaN heterostructure [1–3]. Moreover, high-electron mobility transistors (HEMTs) or metal-insulator-semiconductor HEMTs (MIS-HEMTs) based on the AlGaN/GaN heterojunction have been studied for electronics in the space environments because of a remarkable radiation tolerance of GaN material [4–6]. Electronics used in harsh space environments must be resistant to damage or malfunctions caused by ionizing radiation. In order to evaluate radiation hardness, radiation irradiation effects on the device properties have been explored in MIS-HEMTs with various gate dielectric layers, namely, SiN/Al_2O_3 [7,8], SiN [9,10], Gd_2O_3 [11], MgO/Sc_2O_3 [12], and poly-AlN/SiN [13]. However, these researches have focused on the impact of dielectric on radiation resistance. The impact of the radiation on the performance of GaN devices dependent on the interface between passivation and the GaN layers have not been studied yet. The pre-treatment processes before the deposition passivation layer were applied to improve

the performances of GaN-based devices. In SiN-passivated devices, the pre-treatment process is based on Tetramethylammonium(TMAH) [14], NH_3 [15], H_2SO_4 [16] solutions, and N_2 plasma [17] to enhance SiN/(Al)GaN interface quality because the interface quality affects device performance and reliability. The current collapse characteristics of the AlGaN/GaN heterojunction-based devices can be especially degraded by the surface state of the (Al)GaN layer.

This study evaluated the proton irradiation effect on SiN-passivated MIS-HEMTs that use the TMAH-based pre-treatment process, which was performed to improve the SiN passivation/GaN cap interface quality. To investigate the relationship between the interface conditions and irradiation damage, we analyzed the impact of proton irradiation and the pre-treatment process on the static and dynamic current characteristics of the devices. We also verified the recovery phenomenon of the devices by re-measuring current collapse characteristics after nine months.

2. Device Structure and Fabrication

Figure 1a shows the schematic cross-section of the SiN-passivated AlGaN/GaN MIS-HEMT. The epitaxial structure was created using metal-orgranic chemical vapor deposition (MOCVD) equipment (SYSNEX, Korea) on a sapphire substrate. The device consisted of a 2 μm-thick GaN buffer layer, 60 nm-thick GaN channel layer, 22 nm-thick AlGaN layer, and 2 nm-thick GaN cap layer. Al composition in the AlGaN layer was 0.25. Ssheet charge density of 1.42×10^{13} cm^{-2} and mobility of 1330 $cm^2/V{\cdot}s$ were identified using Hall-effect measurement at room temperature. The overall process flow for the fabrication and proton irradiation is shown in Figure 1b.

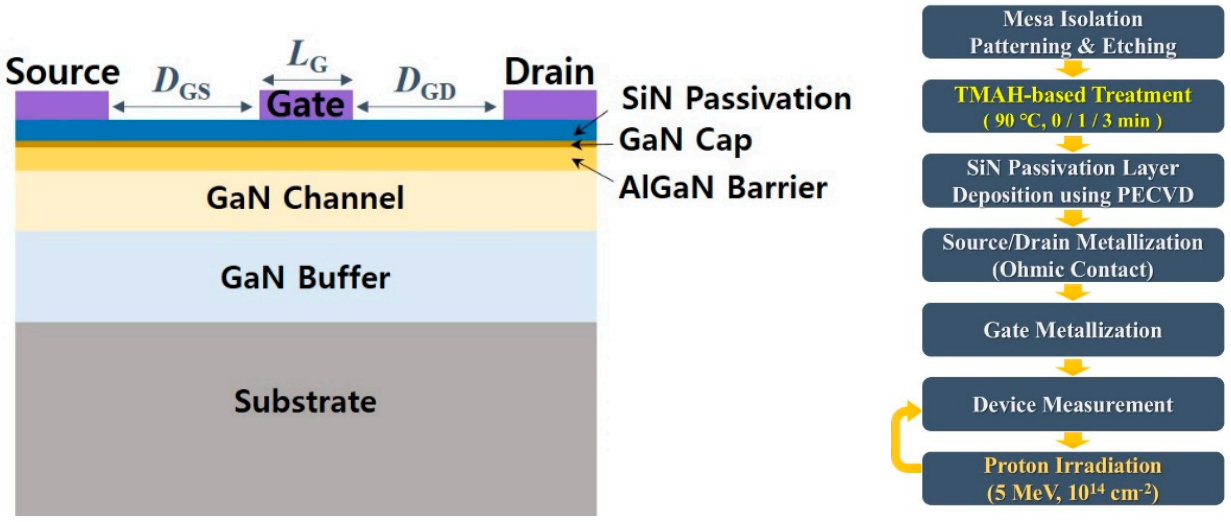

Figure 1. (**a**) Schematic cross-section of the SiN-passivated AlGaN/GaN metal-insulator-semiconductor high-electron mobility transistor (MIS-HEMT). (**b**) Process flow for the fabrication and proton irradiation.

The fabrication began with the dry etching process for electrical isolation between devices. The etched depth was about 250 nm. The wet treatment process based on a TMAH solution (5% concentration) was performed at a temperature of 90 °C. The TMAH solution selectively eliminates Ga atoms on the surface as the alkaline solution and Ga-polar surface is terminated with N atoms after the treatment [18]. Thus, the TMAH-based treatment process influences the removal of native Ga-oxide and enhances the surface roughness [19]. In a previous study, we also confirmed that the TMAH treatment reduced the leakage current characteristics by effectively removing surface states on the GaN cap layer [14]. To investigate effects of the pre-treatment on the surface, we set the treatment time as 0, 1, and 3 min. We used a photoresist developer containing TMAH (AZ 300 MIF) during the photolithography steps. However, the photoresist developer had little impact on the

surface because the TMAH solution reacted with the GaN material at a high temperature of ~90 °C. The TMAH in the photoresist developer was not significantly affected on the surface. We then deposited 20 nm-thick SiN as a passivation and gate dielectric layer using plasma-enhanced chemical vapor deposition (PECVD) (SINIC, Korea) at 370 °C. After the deposition of the SiN layer, source and drain contact were defined by the lithography and electron beam (e-beam) evaporator. After deposition of an Au/Ni/Al/Ti/Si multilayer, the metal layer was annealed using rapid thermal annealing (RTA) at 800 °C for 30 s in a N_2 stmosphere. Finally, Ni/Al/Ni-based metallization was applied for the gate and pad. The current characteristics of completely fabricated devices were measured using a B1500 semiconductor device analyzer (Keysight, Santa Roda, California, USA). The gate length (L_G) and gate-to-source distance (D_{GS}) were 3 μm and 5 μm, respectively. The gate-to-drain distance (D_{GD}) was designed to be 5, 10, 20, and 30 μm. The devices were irradiated by 5 MeV protons with a fluence of 1×10^{14} cm^{-2} using the RFT-30 cyclotron at the Advanced Radiation Technology Institute (ARTI). After proton irradiation, the devices were measured once again. The electrical characteristics of the devices before and after proton irradiation were compared and the effects of proton irradiation and pre-treatment on performances were analyzed. We verified an injection depth of 5 MeV protons using a simulator based on a Monte-Carlo calculation [20]. The protons with 5 MeV energy was injected up to a depth of 125 μm, generating vacancies.

3. Results and Discussion

Figure 2 shows transfer drain current (I_D) and transconductance (g_m)-gate voltage (V_G) characteristics at a drain voltage (V_D) of 10 V of the MIS-HEMT without and with pre-treatment for pre- and post-irradiation. The I_D and g_m characteristics of both the devices slightly decreased.

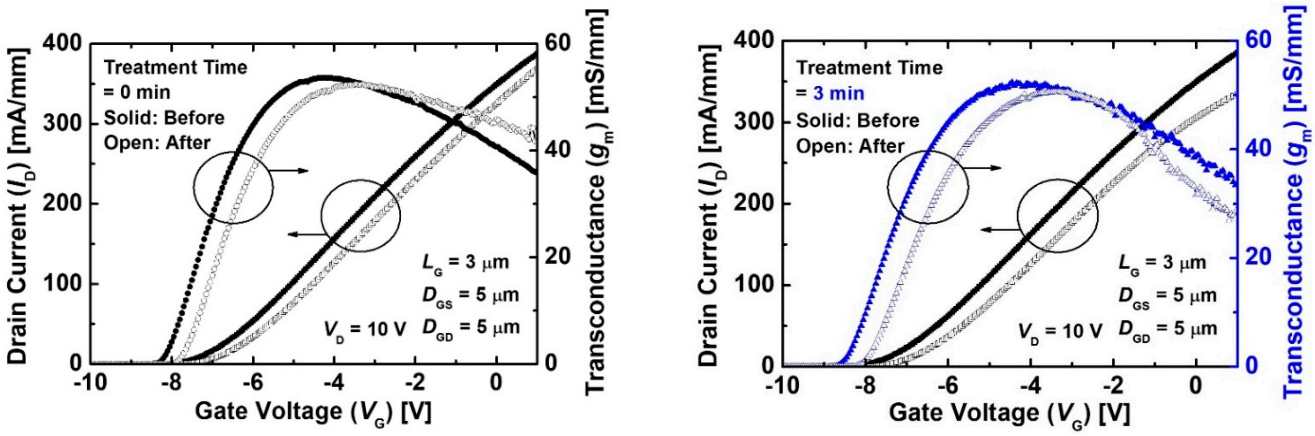

Figure 2. I_D and g_m characteristics as a function of V_G before and after 5 MeV proton irradiation of the MIS-HEMTs (**a**) without treatment and (**b**) with treatment for 3 min at a V_D of 10 V. The L_G, D_{GS}, and D_{GD} of the device were 3, 5, and 5 μm, respectively.

The reduced I_D and g_m was due to the increase in sheet resistance and contact, as shown in Figure 3. The contact and sheet resistances of the devices increased after the proton irradiation because the 2DEG channel and contact were damaged by the injected protons. The proton irradiation generated defects such as Al, Ga, and N vacancies in the 2DEG channel. The defects caused a decrease in electron mobility and 2DEG sheet carrier density [21,22]. More energy loss was in the ohmic contact region due to the heavier mass of the Au atoms. The contact metal as well as the 2DEG region nearby was damaged by more scatter protons from the collisions with heavy atoms [23]. As a result, the increase in the 2DEG channel and contact resistance were caused by radiation-induced defects. A positive shift in threshold voltage (V_{th}) was observed after the proton irradiation. The V_{th}

was defined as the V_G intercept of the linear extrapolation of the I_D at the point of peak g_m (g_{m_max}) [24], and the V_{th} of all the devices were extracted at the I_D-V_G at a low V_D of 0.1 V. The variation rate of the V_{th} values before and after the proton irradiation (ΔV_{th}) of the device without the pre-treatment was about +0.39 V. This is consistent with the results reported in Refs. [8,9]. The proton irradiation induced reduction in electron density within the 2DEG channel due to the displacement damage [25,26]. As a result, the positive shift in V_{th} was caused by the decreased electron density. The device with the treatment also exhibited a V_{th} shift of +0.35 V, as shown in Figure 2b. These results indicate that the 2DEG channel and contact resistances were degraded by the proton irradiation, irrespective of the pre-treatment process.

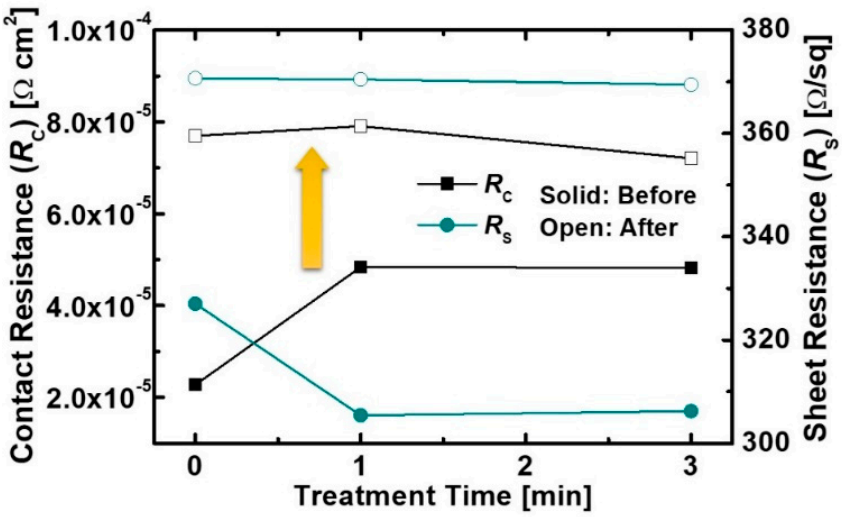

Figure 3. Sheet and contact resistances obtained from the transmission line method (TLM) of samples with and without treatment for 3 min before and after the proton irradiation.

Figure 4a,b show the logarithmic scale I_D and I_G characteristics as a function of V_G before and after the proton irradiation of the MIS-HEMTs with and without the pre-treatment. The off-state currents (I_{off}) of both the devices were reduced more than I_G. The values of I_G were affected by the value of I_{off}. This result indicated that the decrease in I_{off} was affected by the leakage current, except for the I_G. The I_{off} of the MIS-HEMTs was formed by leakage current paths, including a buffer layer and the surface of the mesa-etched region [27,28].

We evaluated the buffer leakage current characteristics by measuring the current between ohmic contacts connecting the mesa-etched region, as shown in Figure 5a. In terms of buffer current characteristics before the irradiation, the structure with the treatment for 3 min was the lowest buffer current because of the enhanced SiN/GaN interface quality effects, as shown in Figure 5b. The buffer current was determined by the currents through the buffer layer and the SiN/GaN interface. A high buffer current of the structure without the treatment was induced by the leakage current path through the SiN/GaN interface, resulting from a large amount of surface states and traps related to the dangling bonds on the etched surface [29]. Because the treatment reduced these defects, the structure with the treatment obtained a relatively low buffer current. The structure with the treatment still exhibited the lowest buffer current of about 10^{-9} A/mm after the proton irradiation. The buffer currents of all structures were reduced to an almost equal rate of about 10^2. This result is due to the defects in the buffer generated by the proton irradiation. Because protons with an identical fluence of 1×10^{14} cm^{-2} were injected into the buffer structure, the proton irradiation generated defects such as Ga vacancies, which increased the resistance of the buffer layer. Consequentially, the decrease in the buffer current led to the reduction in I_{off} of the MIS-HEMTs, as shown in Figure 4.

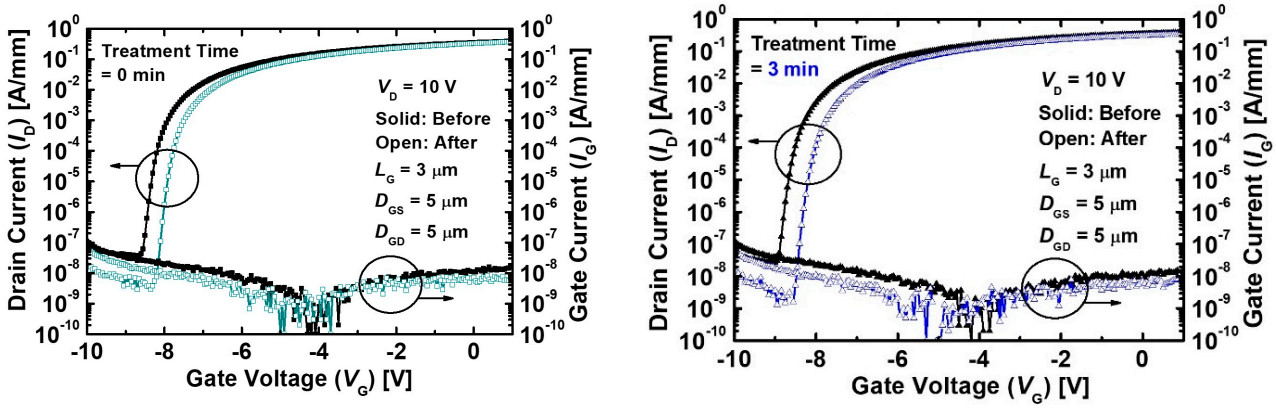

(**a**) (**b**)

Figure 4. I_D and I_G characteristics as a function of V_G before and after the proton irradiation of the MIS-HEMTs (**a**) without the treatment and (**b**) with treatment for 3 min at a V_D of 10 V.

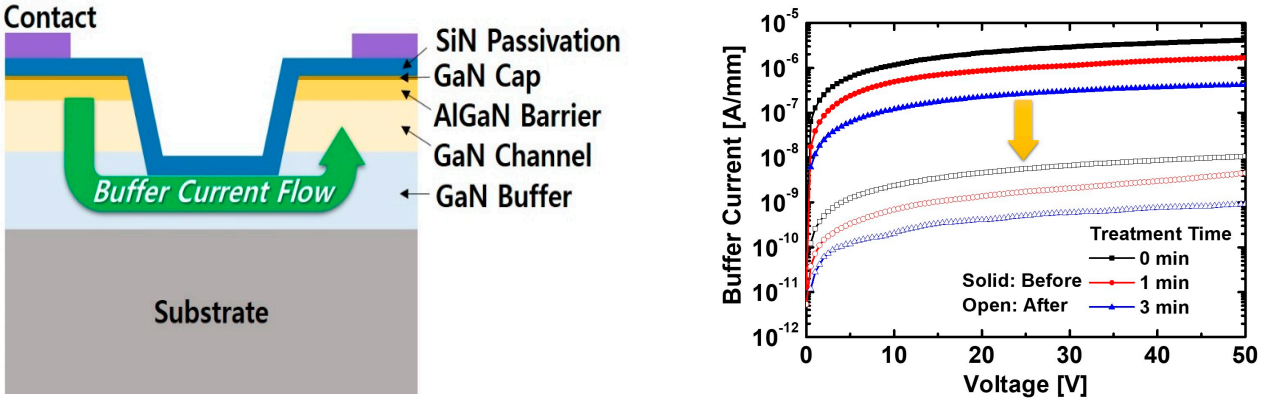

(**a**) (**b**)

Figure 5. (**a**) Schematic structure for measurement of the buffer current. (**b**) Buffer current characteristics of the structure with and without treatment for 1 and 3 min before and after the proton irradiation.

Figure 6a,b show the pulse-mode output I_D-V_D characteristics before and after the proton irradiation of the MIS-HEMTs without and with the treatment. The quiescent bias of the gate and drain (V_{G_B}, V_{D_B}) was 0 V. We verified the output I_D-V_D characteristics at the quiescent bias conditions (V_{G_B}, V_{D_B} = 0 V) to minimize the bias stress and self-heating effect [30]. The pulse period and width (P_{period} and P_{width}) in the pulse-mode measurement were 5 ms and 100 μs, respectively. The I_D of the device after the proton irradiation was lower than that before the proton irradiation. This result was due to a positive shift of V_{th} as well as an increase in sheet and contact resistances. As shown in Figure 6c, all the devices exhibited higher on-resistance (R_{on}) after the proton irradiation than that of the devices before the proton irradiation because of the increased sheet and contact resistances. The variation of R_{on} as a function of D_{GD} exhibited a steep slope because the sheet resistance of the access region became higher [31]. This result was consistent with the transmission line method (TLM) results.

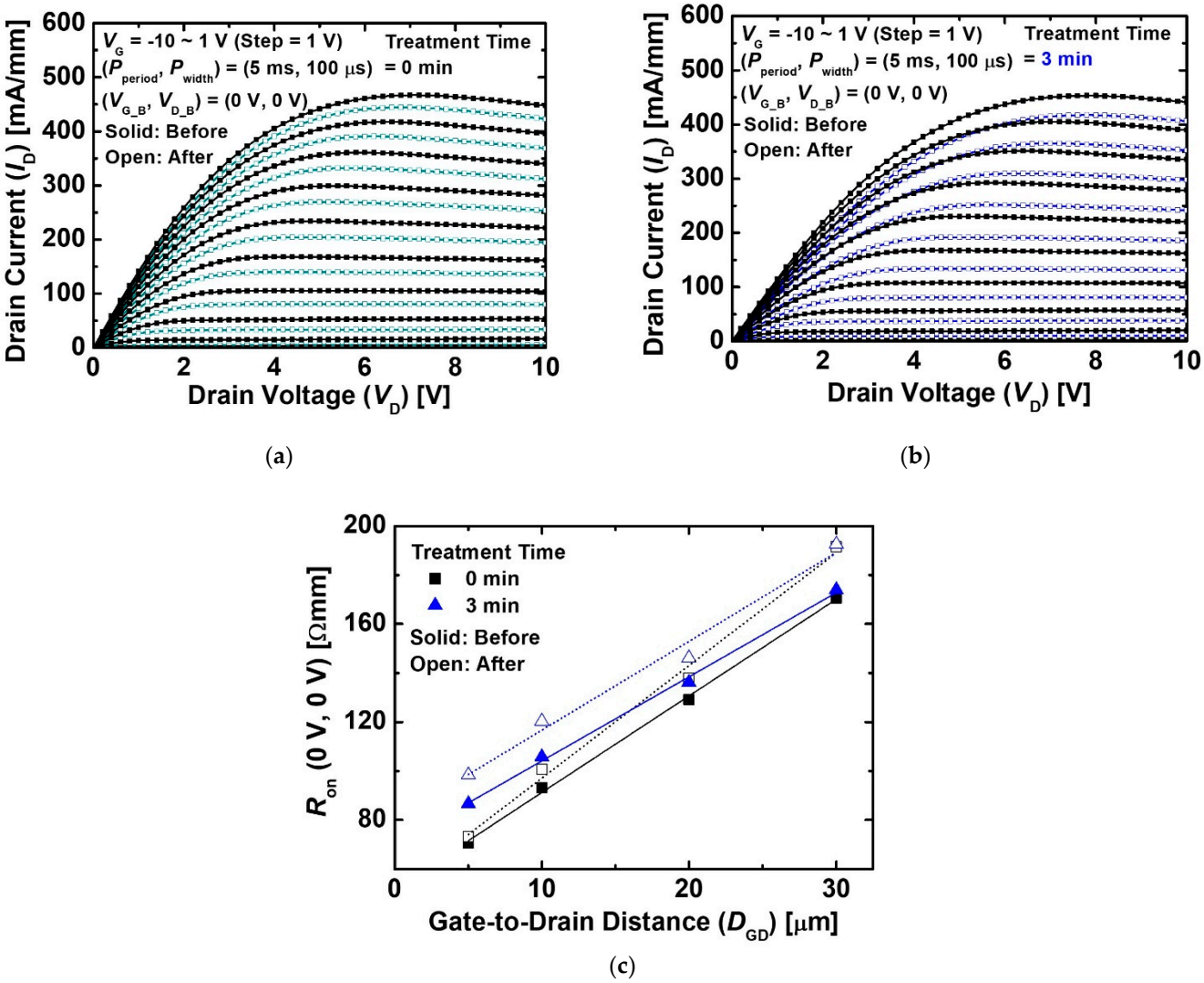

Figure 6. Pulse-mode output I_D-V_D characteristics of the MIS-HEMTs (**a**) without treatment and (**b**) with treatment for 3 min before and after the proton irradiation. The L_G, D_{GS}, and D_{GD} of the device was 3, 5, and 5 μm, respectively. (**c**) Variation of R_{on} as a function of D_{GD}. The V_{G_B} and V_{D_B} were 0 V. The P_{period} and P_{width} were 5 ms and 100 μs, respectively.

Figure 7a exhibits the current collapse characteristics of the MIS-HEMTs before and after the proton irradiation. The quiescent biases of the gate and drain (V_{G_B}, V_{D_B}) were (0 V, 0 V), (−10 V, 0 V), (0 V, 20 V), and (−10 V, 20 V). The pulse period and width (P_{period} and P_{width}) were 5 ms and 100 μs, respectively. Before proton irradiation, the device with the pre-treatment exhibited a relatively less impact of gate bias stress on the current characteristics because of a better quality of the SiN/GaN interface. However, as the pre-treatment time increased, the gate-lag characteristics degenerated after the proton irradiation. As shown in Figure 7b, the R_{on} variation of the device with the pre-treatment for 3 min were significantly increased by the irradiation. The device with the pre-treatment for 3 min exhibited more damaged on the device surface with the irradiation, as shown in the microscopic image of Figure 7c. Compared to the gate-lag characteristics, the current characteristics of all the devices were hardly changed by the drain bias stress condition. These results indicated that the SiN/GaN interface was affected by the proton irradiation. The TMAH-based pre-treatment removed native Ga-oxide from the surface of the GaN cap layer and the surface became N-terminated. The adsorption of hydrogen can be enhanced by the N-terminated surface [32,33]. During the SiN deposition process, the surface was covered by the hydrogen in SiH_4 or NH_3 [34]. The hydrogen between the SiN/GaN interface was removed by the proton irradiation, which may generate high temperature

or displacement damage. The removal of hydrogen passivation in the SiN/GaN interface forms defects and degenerates gate-lag characteristics.

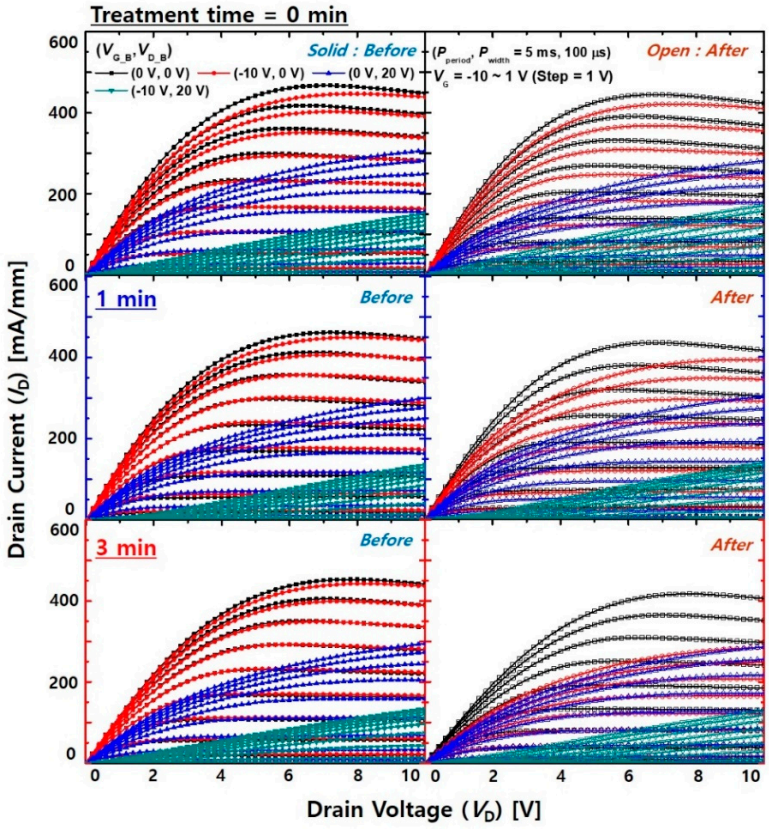

(**a**)

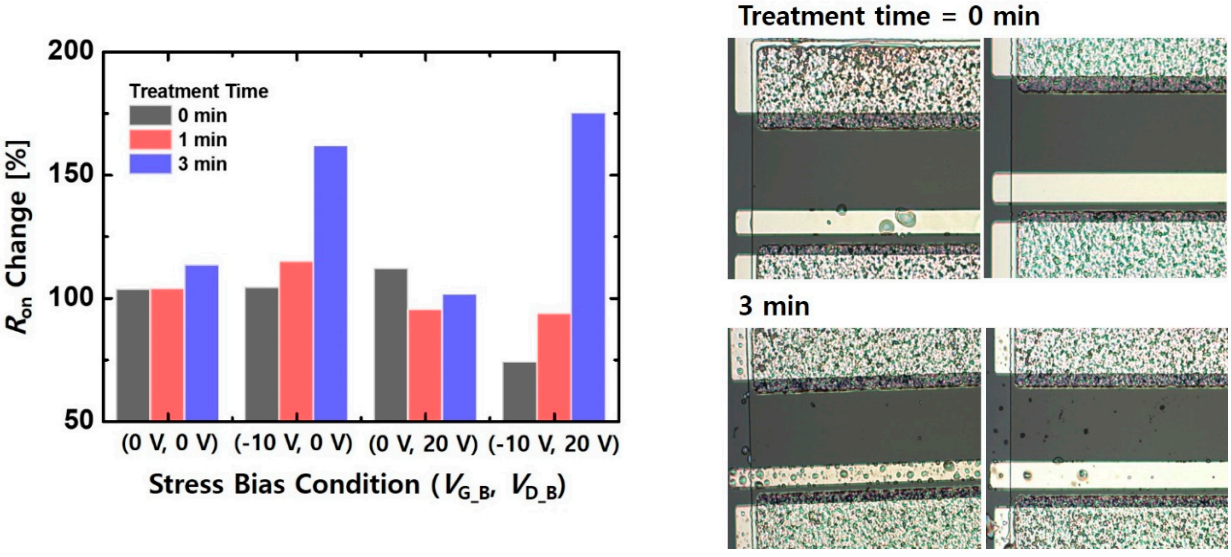

(**b**) (**c**)

Figure 7. (**a**) Current collapse characteristics of the MIS-HEMTs before and after proton irradiation. (**b**) Variation rates of R_{on} depending on different stress bias conditions. The V_{G_B} and V_{D_B} were (0 V, 0 V), (−10 V, 0 V), (0 V, 20 V), and (−10 V, 20 V). The P_{period} and P_{width} were 5 ms and 100 µs, respectively. The L_G, D_{GS}, and D_{GD} of the device were 3, 5, and 5 µm, respectively. (**c**) Optical microscope image after irradiation of the devices with and without treatment.

As shown in Figure 8a, MIS-HEMTs with pre-treatment for 3 min exhibited a large increase in the rate in terms of gate-lag characteristics dependent on D_{GD}. As D_{GD} increased, the device exhibited a high variation in resistance because the impact of the drain bias on trapped electrons near the gate edge was reduced by a long D_{GD}. Figure 8b shows the drain-lag characteristics of the MIS-HEMTs before and after the proton irradiation as a function of D_{GD}. All the devices obtained a low variation rate of R_{on} after the proton irradiation because the R_{on} at $V_{G\_B} = V_{D\_B} = 0$ V was largely degraded more than R_{on} at $V_{G\_B} = V_{D\_B} = 10$ V.

Figure 9a shows the I_D and g_m characteristics as a function of V_G of the device with the pre-treatment for 3 min before and after proton irradiation and nine months after the irradiation. We stored the devices in an ambient atmosphere for nine months. The degenerated I_D and g_m increased after nine months while V_{th} was hardly changed. Because the g_m value is associated with channel mobility [35], the current characteristics were largely recovered by the recovered mobility. The unchanged V_{th} means no change in the 2DEG density. The gate-lag characteristics recovered over time, as shown in Figure 9b. These results indicated that the damaged SiN/GaN interface was reconstructed by the re-passivation of hydrogen. Hydrogen was diffused from SiN or the atmosphere to the SiN/GaN interface, and formed hydrogenated vacancies. The hydrogen from SiN and the hydrogen were able to recover the proton irradiation-generated defects [36]. Thus, the performance of the devices with the pre-treatment irradiated by the protons were recovered by the hydrogen passivation effects.

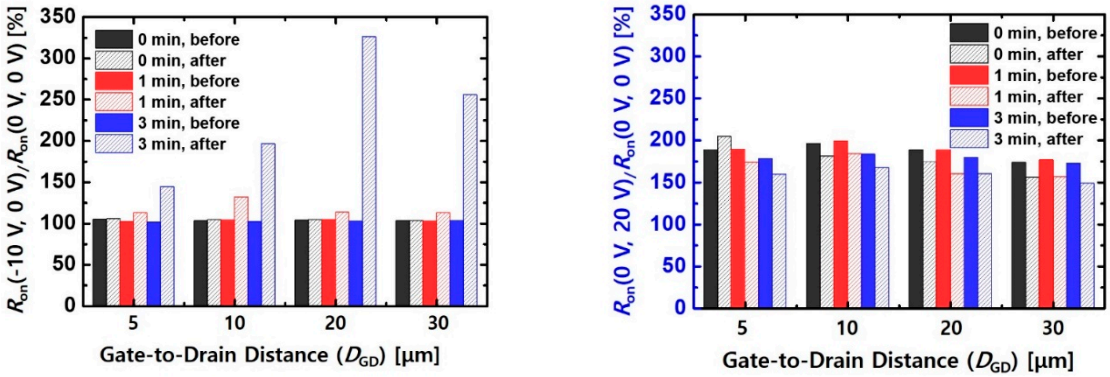

(**a**) (**b**)

Figure 8. Variation in rates of R_{on} depending on (**a**) gate and (**b**) drain stress bias conditions of the MIS-HEMTs with different values of D_{GD}. The P_{period} and P_{width} were 5 ms and 100 μs, respectively.

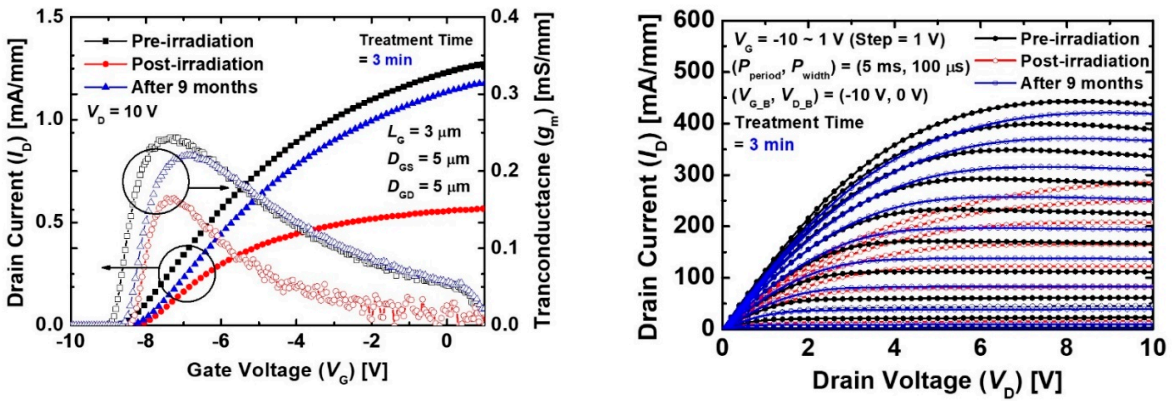

(**a**) (**b**)

Figure 9. (**a**) I_D and g_m characteristics as a function of V_G at a low V_D of 0.1 V and (**b**) gate-lag characteristics of the MIS-HEMTs with treatment for 3 min before and after irradiation, and after nine months.

4. Conclusions

We studied the effects of proton irradiation on SiN-passivated AlGaN/GaN MIS-HEMTs with a TMAH-based pre-treatment process for a fixed fluence of 1×10^{14} cm^{-2} at a proton energy of 5 MeV. The static I_D characteristics of the devices decreased regardless of the implementation of a pre-treatment process because the increase in sheet and contact resistances was caused by radiation damage. The gate-lag characteristics of the device with the pre-treatment was remarkably degenerated after proton irradiation. The hydrogen in the SiN/GaN interface formed by the TMAH-based pre-treatment and SiN deposition process was removed by the injected protons. As a result, the degeneration of the gate-lag characteristics was induced by the generated vacancies. After nine months, the current and gate-lag characteristics of the device with pre-treatment were recovered by the hydrogen re-passivation. The results of this study confirmed that the conditions of the SiN/GaN interface affected the radiation hardness of SiN-passivated MIS-HEMTs.

Author Contributions: Conceptualization, Y.J.Y. and D.S.K.; Investigation, Y.J.Y.; data analysis, Y.J.Y., J.S.L., J.K.S., I.M.K., J.H.L., E.J.L. and D.S.K.; writing—original draft preparation, Y.J.Y.; writing—review and editing, D.S.K. All authors have read and agreed to the published version of the manuscript.

Funding: This work was supported by the KOMAC (Korea Multi-purpose Accelerator Complex) operation fund of KAERI (Korea Atomic Energy Research Institute) and the National Research Foundation of Korea (No.2018R1D1A1B07051027) by MSIT (Ministry of Science and ICT).

Conflicts of Interest: The authors declare no conflict of interest.

References

1. Mishra, U.K.; Parikh, P.; Wu, Y.-F. AlGaN/GaN HEMTs-an overview of device operation and applications. *Proc. IEEE* **2002**, *90*, 1022–1031. [CrossRef]
2. Ikeda, N.; Niiyama, Y.; Kambayashi, H.; Sato, Y.; Nomura, T.; Kato, S.; Yoshida, S. GaN Power Transistors on Si Substrates for Switching Applications. *Proc. IEEE* **2010**, *98*, 1151–1161. [CrossRef]
3. Baliga, B.J. Gallium nitride devices for power electronic applications. Semicond. *Sci. Technol.* **2013**, *28*, 074011.
4. Ionascut-Nedelcescu, A.; Carlone, C.; Houdayer, A.; Bardeleben, H.J.; Cantin, J.-L.; Raymond, S. Radiation hardness of gallium nitride. *IEEE Trans. Nucl. Sci.* **2002**, *49*, 2733–2738. [CrossRef]
5. Pearton, S.; Ren, F.; Patrick, E.; Law, M.E.; Polyakov, A.Y. Review—Ionizing Radiation Damage Effects on GaN Devices. *ECS J. Solid State Sci. Technol.* **2016**, *5*, Q35–Q60. [CrossRef]
6. Weaver, B.D.; Anderson, T.J.; Koehler, A.D.; Greenlee, J.D.; Hite, J.; Shahin, D.I.; Kub, F.J.; Hobart, K.D. Editors' Choice—On the Radiation Tolerance of AlGaN/GaN HEMTs. *ECS J. Solid State Sci. Technol.* **2016**, *5*, Q208–Q212. [CrossRef]
7. Chang, S.-H.; Cho, K.J.; Jung, H.-W.; Kim, J.-J.; Jang, Y.-J.; Bae, S.-B.; Kim, D.-S.; Bae, Y.; Yoon, H.S.; Ahn, H.-K.; et al. Improvement of Proton Radiation Hardness Using ALD-Deposited Al2O3 Gate Insulator in GaN-Based MIS-HEMTs. *ECS J. Solid State Sci.* **2019**, *8*, Q245–Q248. [CrossRef]
8. Lee, J.-H.; Kim, D.-S.; Kim, J.-G.; Ahn, W.-H.; Bae, Y.; Lee, J.-H. Effect of gate dielectrics on characteristics of high-energy proton-irradiated AlGaN/GaN MISHEMTs. *Radiat. Phys. Chem.* **2021**, *184*, 109473. [CrossRef]
9. Fares, C.; Ren, F.; Pearton, S.; Yang, G.; Kim, J.; Lo, C.-F.; Johnson, J.W. Effect of proton irradiation energy on SiNx/AlGaN/GaN metal-insulator semiconductor high electron mobility transistors. *J. Vac. Sci. Technol. B* **2018**, *36*, 052202. [CrossRef]
10. Gao, Z.; Romero, M.F.; Redondo-Cubero, A.; Pampillon, M.A.; Andres, E.S.; Calle, F. Effects of Gd_2O_3 Gate Dielectric on Proton-Irradiated AlGaN/GaN HEMTs. *IEEE Electron Device Lett.* **2017**, *38*, 611–614. [CrossRef]
11. Luo, B.; Ren, F.; Allums, K.; Gila, B.; Onstine, A.; Abernathy, C.; Pearton, S.; Dwivedi, R.; Fogarty, T.; Wilkins, R.; et al. Proton irradiation of MgO- or Sc2O3 passivated AlGaN/GaN high electron mobility transistors. *Solid State Electron.* **2003**, *47*, 1015–1020. [CrossRef]
12. Zhang, D.; Cheng, X.; Shen, L.; Zheng, L.; Gu, Z.; Zhou, W.; Liu, X.; Yu, Y. Influence of Poly-AlN Passivation on the Perfor-mance Improvement of 3-MeV Proton-Irradiated AlGaN/GaN MIS-HEMTs. *IEEE Trans. Nucl. Sci.* **2019**, *66*, 2215–2219. [CrossRef]
13. He, J.; Feng, M.; Zhong, Y.; Wang, J.; Zhou, R.; Gao, H.; Zhou, Y.; Sun, Q.; Liu, J.; Huang, Y.; et al. On-wafer fabrication of cavity mirrors for InGaN-based laser diode grown on Si. *Sci. Rep.* **2018**, *8*, 7922. [CrossRef] [PubMed]
14. Yoon, Y.J.; Seo, J.H.; Cho, M.S.; Kang, H.-S.; Won, C.-H.; Kang, I.M.; Lee, J.-H. TMAH-based wet surface pre-treatment for reduction of leakage current in AlGaN/GaN MIS-HEMTs. *Solid State Electron.* **2016**, *124*, 54–57. [CrossRef]
15. Edwards, A.; Mittereder, J.; Binari, S.; Katzer, D.; Storm, D.; Roussos, J. Improved reliability of AlGaN-GaN HEMTs using an NH/sub 3/ plasma treatment prior to SiN passivation. *IEEE Electron Device Lett.* **2005**, *26*, 225–227. [CrossRef]
16. Zaidi, Z.H.; Lee, K.B.; Guiney, I.; Qian, H.; Jiang, S.; Wallis, D.J.; Humphreys, C.J.; Houston, P.A. Sulfuric acid and hydro-gen peroxide surface passivation effects on AlGaN/GaN high electron mobility transistors. *J. Appl. Phys.* **2014**, *116*, 244501. [CrossRef]

17. Romero, M.; Brana, A.; Cuerdo, R.; Jimenez, A.; Miguel-Sanchez, J.; Gonzalez-Posada, F.; Gomez, F.C.; Munoz, E. Effects of N2N2 Plasma Pretreatment on the SiN Passivation of AlGaN/GaN HEMT. *IEEE Electron Device Lett.* **2008**, *29*, 209–211. [CrossRef]
18. Reddy, M.S.P.; Park, W.-S.; Im, K.-S.; Lee, J.-H. Dual-Surface Modification of AlGaN/GaN HEMTs Using TMAH and Piranha Solutions for Enhancing Current and 1/f-Noise Characteristics. *IEEE J. Electron Devices Soc.* **2018**, *6*, 791–796. [CrossRef]
19. Kim, K.-W.; Jung, S.-D.; Kim, D.-S.; Kang, H.-S.; Im, K.-S.; Oh, J.-J.; Ha, J.-B.; Shin, J.-K.; Lee, J.-H. Effects of TMAH Treatment on Device Performance of Normally Off Al2O3/GaN MOSFET. *IEEE Electron Device Lett.* **2011**, *32*, 1376–1378. [CrossRef]
20. Ziegler, J.F.; Ziegler, M.; Biersack, J. SRIM – The stopping and range of ions in matter (2010). *Nucl. Instrum. Methods Phys. Res. Sect. B Beam Interact. Mater. Atoms* **2010**, *268*, 1818–1823. [CrossRef]
21. Polyakov, A.Y.; Pearton, S.; Frenzer, P.; Ren, F.; Liu, L.; Kim, J. Radiation effects in GaN materials and devices. *J. Mater. Chem. C* **2012**, *1*, 877–887. [CrossRef]
22. Auret, F.D.; Goodman, S.A.; Koschnick, F.K.; Spaeth, J.-M.; Beaumont, B.; Gibart, P. Proton bombardment-induced electron traps in epitaxially grown n-GaN. *Appl. Phys. Lett.* **1999**, *74*, 407–409. [CrossRef]
23. Liu, L.; Cuervo, C.V.; Xi, Y.; Ren, F.; Pearton, S.J.; Kim, H.-Y.; Kim, J.; Kravchenko, I.I. Impact of proton irradiation on dc performance of AlGaN/GaN high electron mobility transistors. *J. Vac. Sci. Technol. B* **2013**, *31*, 042202. [CrossRef]
24. Cai, Y.; Zhou, Y.; Lau, K.M.; Chen, K.J. Control of Threshold Voltage of AlGaN/GaN HEMTs by Fluoride-Based Plasma Treatment: From Depletion Mode to Enhancement Mode. *IEEE Trans. Electron Devices* **2006**, *53*, 2207–2215. [CrossRef]
25. Greenlee, J.D.; Specht, P.; Anderson, T.J.; Koehler, A.D.; Weaver, B.D.; Luysberg, M.; Dubon, O.D.; Kub, F.J.; Weatherford, T.R.; Hobart, K.D. Degradation mechanisms of 2 MeV proton irradiated AlGaN/GaN HEMTs. *Appl. Phys. Lett.* **2015**, *107*, 083504. [CrossRef]
26. Kim, D.-S.; Lee, J.-H.; Kim, J.-G.; Yoon, Y.J.; Lee, J.S.; Lee, J.-H. Anomalous DC Characteristics of AlGaN/GaN HEMTs De-pending on Proton Irradiation Energies. *ECS J. Solid State Sci.* **2020**, *9*, 065005. [CrossRef]
27. Lin, Y.-S.; Lain, Y.-W.; Hsu, S. AlGaN/GaN HEMTs with Low Leakage Current and High On/Off Current Ratio. *IEEE Electron Device Lett.* **2009**, *31*, 102–104. [CrossRef]
28. Xu, Z.; Wu, W.; Ma, X.; Zhang, J.; Hao, Y.; Wang, J.; Cai, Y.; Liu, J.; Jin, C.; Yang, Z.; et al. Enhancement Mode (E-Mode) AlGaN/GaN MOSFET With 10−1310−13 A/mm Leakage Current and 10121012 ON/OFF Current Ratio. *IEEE Electron Device Lett.* **2014**, *35*, 1200–1202. [CrossRef]
29. Liu, Z.H.; Ng, G.I.; Zhou, H.; Arulkumaran, S.; Maung, Y.K.T. Reduced surface leakage current and trapping effects in Al-GaN/GaN high electron mobility transistors on silicon with SiN/Al_2O_3 passivation. *Appl. Phys. Lett.* **2011**, *98*, 113506. [CrossRef]
30. Wang, X.-D.; Hu, W.-D.; Chen, X.-S.; Lu, W. The Study of Self-Heating and Hot-Electron Effects for AlGaN/GaN Dou-ble-Channel HEMTs. *IEEE Trans. Electron Devices* **2012**, *59*, 1393–1401. [CrossRef]
31. Ohi, K.; Asubar, J.; Nishiguchi, K.; Hashizume, T. Current Stability in Multi-Mesa-Channel AlGaN/GaN HEMTs. *IEEE Trans. Electron Devices* **2013**, *60*, 2997–3004. [CrossRef]
32. Northrup, J.E.; Neugebauer, J. Strong affinity of hydrogen for the GaN(000-1) surface: Implications for molecular beam epitaxy and metalorganic chemical vapor deposition. *Appl. Phys. Lett.* **2004**, *85*, 3429–3431. [CrossRef]
33. Wang, Y.-L.; Ren, F.; Zhang, U.; Sun, Q.; Yerino, C.D.; Ko, T.S.; Cho, Y.S.; Lee, I.H.; Han, J.; Pearton, S.J. Improved hydro-gen detection sensitivity in N-polar GaN Schottky diodes. *Appl. Phys. Lett.* **2009**, *94*, 212108. [CrossRef]
34. Lelievre, J.-F.; Fourmond, E.; Kaminski, A.; Palais, O.; Ballutaud, D.; Lemiti, M. Study of the composition of hydrogenated silicon nitride SiNx:H for efficient surface and bulk passivation of silicon. *Sol. Energy Mater. Sol. Cells* **2009**, *93*, 1281–1289. [CrossRef]
35. Vitanov, S.; Palankovski, V.; Maroldt, S.; Quay, R.; Murad, S.; Rodle, T.; Selberherr, S. Physics-Based Modeling of GaN HEMTs. *IEEE Trans. Electron Devices* **2012**, *59*, 685–693. [CrossRef]
36. Chen, Z.; Yue, S.; Peng, C.; Zhang, Z.; Liu, C.; Wang, L.; Huang, Y.; Huang, Y.; He, Y.; Zhong, X.; et al. Hydrogen-Related Recovery Effect of AlGaN/GaN High-Electron-Mobility Transistors Irradiated by High-Fluence Protons. *IEEE Trans. Nucl. Sci.* **2021**, *68*, 118–123. [CrossRef]